Materials Transactions, Vol. 53, No. 7 (2012) pp. 1247 to 1251

First-Principles Calculations on Elasticity and Anisotropy of Tetragonal Tungsten Dinitride under Pressure

Hongcun Zhai[1], Xiaofeng Li[2,*] and Junyi Du[1]

[1]*Mathematics College, Luoyang Normal College, Henan Luoyang 471022, P. R. China*
[2]*College of Physics and Electronic Information, Luoyang Normal College, Henan Luoyang, 471022, P. R. China*

First-principles calculations of the crystal structure and the elastic properties of tetragonal WN_2 have been performed with the plane-wave pseudopotential density functional theory method. The calculated structural parameters and elastic constants at zero pressure and temperature are in excellent agreement with the available theoretical results. The dependence of the elastic constants C_{ij}, the aggregate elastic moduli B, G and the anisotropies on pressure have been investigated. WN_2 is a brittle system below about 66 GPa, whereas it becomes ductile under high pressure. By the elastic stability criteria, it is predicted that tetragonal WN_2 are not stable above 232.1 GPa.
[doi:10.2320/matertrans.M2011373]

(Received December 2, 2011; Accepted March 23, 2012; Published June 25, 2012)

Keywords: *elastic properties, anisotropy, WN_2*

1. Introduction

Superhard materials are of great importance in science and technology, with applications in abrasives, coatings, cutting, polishing tools, etc. Hardness, in general, is understood as the extent which a given solid resists both elastic and plastic deformations.[1)] Recently, platinum, iridium, and osmium dinitrides were successfully synthesized under pressure and temperature, which could be quenched and stabilized to ambient conditions.[2–4)] The anomaly of these nitrides have low compressibility, comparable to that of *c*-BN, which suggests that they are potential superhard materials. Meanwhile, many theoretical investigations have been performed to explore their structures, which is very important to determine their physical properties. For PtN_2, first-principles calculations show that it should have a pyrite structure,[5)] which agrees well with the experiment.[3)] The space groups of OsN_2 and IrN_2[3,6)] were also identified by theoretical calculations as orthorhombic *Pnnm* and monoclinic $P121/c1$ structures, respectively.

However, to date, WN_2 have not been synthesized in crystalline form. Peter Kroll *et al.*[7)] proposed two structures of baddeleyite and cotunnite types which are superior to the fluorite-type structure. Two hexagonal $P6_3/mmc$ and P-$6m2$ structures[8,9)] of WN_2 with N–W–N "sandwiches" layers, which are more stable than the cotunnite and baddeleyite ones, are predicted by the first-principles calculations. The elastic properties of two hexagonal structures are also explored.[9)] The mechanical stability and elastic properties of hexagonal structures of WN_2 under pressure are investigated by density function theory.[10)] The structural properties of tetragonal WN_2 and ReN_2[11)] at zero pressure are studied from first-principles calculations. They found that tetragonal phase in WN_2 should be stable above 175 GPa. Although they think that tetragonal WN_2 may be difficult to be synthesized, the calculated shear modulus of tetragonal WN_2 is largest in the all synthesized $5d$ transition metal dinitrides. For the partially covalent transition metal-based hard materials, shear modulus has been considered as a very important parameter, governing the indentation hardness. It is therefore valuable to investigate the physical properties of tetragonal WN_2, which have important guiding significances to the investigation of other similar compounds. Thus, in the present work, we investigate the elastic properties and the anisotropies of WN_2 under pressure by using the plane-wave pseudopotential density functional theory. In Section 2, we have made a brief review of the theoretical method. The results and some discussions are presented in Section 3.

*Corresponding author, E-mail: lxfdjy@126.com

2. Theory Method

First principle calculations, based on the density functional theory (DFT), have shown a good accuracy in the study of many physical and chemical properties for a wide scale of materials. The CASTEP (Cambridge Serial Total Energy Package) code[12)] was used for these calculations. The total energy electronic structure calculations were performed using the plane-wave pseudopotential technique within the density functional theory. The non-local ultrasoft pseudopotential (USPP) introduced by Vanderbilt[13)] was employed for all ion–electron interactions. The structures were relaxed using the Broyden, Fletcher, Goldfarb and Shannon (BFGS) minimization method algorithm. To compare the performance of different approximations of exchange–correlation interaction, we adopted both the local density approximation (LDA-CAPZ) proposed by Vosko, Wilk and Nussair[14)] for the approximations of exchange–correlation interactions. The electronic wave functions are expanded in a plane wave basis set with energy cut-off of 500 eV. Pseudo-atom calculations are performed for N $2s^2$ $2p^3$ and W $5s^2$ $5p^6$ $5d^4$ $6s^2$. For the Brillouin-zone k-point sampling, we use the Monkhorst–Pack mesh with $10 \times 10 \times 8$ k points. In geometrical relaxations, the self-consistent convergence total energy of the system converged to within 1.0×10^{-7} eV/atom. The maximum tolerance was less than 5×10^{-6} eV/atom for the energy, and less than 1.0×10^{-2} eV/atom for the force. These parameters are sufficient in leading to well converged total energy and geometrical configurations.

To calculate the elastic constants under hydrostatic pressures, we employ the strains to be non-volume conserving. The elastic constants C_{ijkl} with respect to the finite strain variables are then determined as:[15–17]

$$c_{ijkl} = \left(\frac{\partial \sigma_{ij}(x)}{\partial e_{kl}}\right)_X \tag{1}$$

where s_{ij} and e_{kl} are the applied stress and Eulerian strain tensors, and X and x are the coordinates before and after the deformation. For the isotropic stress, the elastic constants are defined as:[16–18]

$$c_{ijkl} = C_{ijkl} + \frac{P}{2}(2\delta_{ij}\delta_{kl} - \delta_{il}\delta_{jk} - \delta_{ik}\delta_{jl}) \tag{2}$$

$$C_{ijkl} = \left(\frac{1}{V(x)}\frac{\partial^2 E(x)}{\partial e_{ij}\partial e_{kl}}\right)_X \tag{3}$$

where C_{ijkl} is the second-order derivatives with respect to the infinitesimal strain (Eulerian). The fourth-rank tensor C has generally 21 independent components. However, this number is greatly reduced when considering the symmetry of the crystal. For tetragonal crystals WN_2, there are six independent components of elastic constants, i.e. C_{11}, C_{33}, C_{44}, C_{66}, C_{12} and C_{13}.

According to the Voigt approximation[19] there is a simple relation between the isotropic bulk moduli B_V and shear moduli G_V of a polycrystalline aggregate and the single-crystal elastic constants C_{ij}:

$$B_V = \frac{1}{9}[2(C_{11} + C_{12}) + C_{33} + 4C_{13}] \tag{4}$$

$$G_V = \frac{1}{30}(M + 3C_{11} - 3C_{12} + 12C_{44} + 6C_{66}) \tag{5}$$

$$M = (C_{11} + C_{12}) + 2C_{33} - 4C_{13} \tag{6}$$

Reuss[20] derived a linear relation between the isotropic bulk B_R and shear moduli G_R of a polycrystalline aggregate are defined as follows:

$$B_R = C^2/M \tag{7}$$

$$G_R = 15/((18B_V)/C^2 + 6/(C_{11} - C_{12}) + 6/C_{44} + 3/C_{66}) \tag{8}$$

$$C^2 = (C_{11} + C_{12})C_{33} - 2C_{13}^2 \tag{9}$$

Hill[21] proved that the Voigt and Reuss equations represent upper and lower limits of the true polycrystalline constants. It showed that the polycrystalline moduli are the arithmetic mean values of the Voigt and Reuss moduli and thus obtained by

$$B = (B_V + B_R)/2 \quad G = (G_V + G_R)/2 \tag{10}$$

3. Results and Discussions

For the potential superhard material tetragonal WN_2, the total energy electronic structure calculations are performed in a wide range of primitive cell volumes V, i.e., from $0.75V_0$ to $1.3V_0$, where V_0 is the zero pressure equilibrium primitive cell volume. No constraints are imposed on the c/a ratio, i.e., both lattice parameter a and c are optimized simultaneously. It is found from our calculations that the most stable structure of tetragonal WN_2 occurs at the axial ratio $c/a = 2.735$, corresponding to the equilibrium lattice constants: $a = 2.664$ Å, $c = 7.285$ Å. By fitting the obtained E–V data by the Birch–Murnaghan equation of state,[22] the bulk modulus B_0 and its pressure derivative B_0', bond length of N–N, W–N are also listed in Table 1, together with the available theoretical data.[11] Generally, high hardness materials have large bulk modulus. The bulk modulus B represents the resistance to fracture. From Table 1, the calculated bulk modulus B_0 of tetragonal WN_2 is 421.4 GPa within LDA, which is between those of the superhard material c-BN (369–382 GPa)[23] and diamond (446 GPa),[24] and higher than that of ReB_2 of 354 GPa within LDA (326 GPa within GGA),[25] OsN_2 of 417 GPa within LDA (359 GPa within GGA),[26] which indicates that tetragonal WN_2 is also candidates of ultra-incompressible materials.

Table 1 The calculated equilibrium parameter a (Å), c (Å), bulk modulus B_0 (GPa) and pressure derivative bulk modulus B_0', bond length of N–N, W–N (Å) with available theoretical data.

	a	c	c/a	B_0	B_0'	N–N	W–N
Present	2.664	7.285	2.735	421.4	4.51	1.404	2.191
LDA[11]	2.67	7.28		429	4.49	1.39	2.20
GGA[11]	2.71	7.38		378	4.58	1.41	2.23

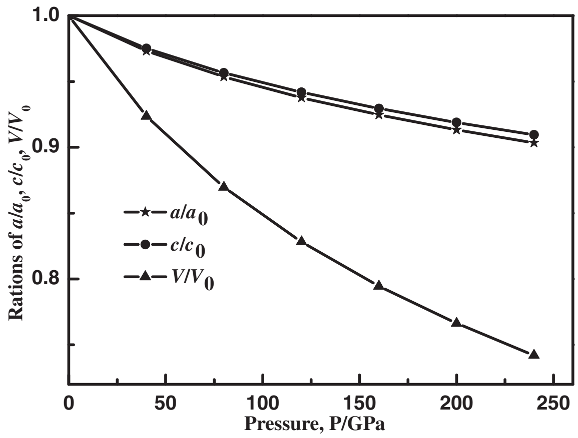

Fig. 1 Normalized parameters a/a_0, c/c_0, and V/V_0 as a function of pressure at $T = 0$.

The pressure dependence of the normalized lattice parameters a/a_0, c/c_0 and the normalized cell volume V/V_0 (where a_0, c_0 and V_0 are the zero pressure equilibrium structure parameters) are illustrated in Fig. 1. It is shown that, below 10 GPa, a small difference in fractional axis compression value appears; as pressure increases, the equilibrium ratio a/a_0 decreases more quickly than that of c/c_0, indicating that compression along c-axis is more difficult than that along a-axis. Unfortunately, there are no experimental data to be compared with our data.

The six elastic constants C_{11}, C_{33}, C_{44}, C_{66}, C_{12} and C_{13} of tetragonal WN_2 at 0 GPa and 0 K are listed in Table 2. There is currently no experimental measurement of elastic constants for our comparison. However, our results are well consistent with those by Du *et al.*[11] The mechanical stability of a crystal implies that the strain energy must be positive. Obviously, the elastic constants of WN_2 crystal obey the mechanical stability criteria of the tetragonal structure:

$$C_{11} - C_{12} > 0 \quad C_{11} + C_{33} - 2C_{13} > 0$$
$$C_{ii} > 0 \ (i = 1, 3, 4, 6)$$
$$2C_{11} + C_{33} + 2C_{12} + 4C_{13} > 0 \tag{11}$$

which indicates tetragonal WN_2 is stable at 0 K and 0 GPa.

The pressure dependence of elastic constants of WN_2 (up to 240 GPa) is summarized in Table 3. In the present calculations, $C_{11} > C_{33}$, which exhibited that the bonding strength along the [100] and [010] direction is stronger than that of the bonding along the [001] direction. $C_{44} < C_{66}$, it indicated that the [100] (010) shear is more difficult than the [100] (001) shear. The [ijk] and (ijk) denote symmetry axis and plane, respectively. It is also clearly found that C_{11}, C_{33}, C_{66}, C_{12} and C_{13} are susceptible to pressure, while, and C_{44} varies little under the effect of pressure. Moreover, C_{44} firstly increases and subsequently decreases with pressure.

High bulk modulus is not enough to describe the mechanical strength of a material. Shear modulus is a significantly better qualitative predictor of hardness than the bulk modulus. Moreover, the material is often used as polycrystalline aggregates, and therefore it is useful to estimate the corresponding parameters of the polycrystalline species. Therefore, the bulk modulus B and shear modulus G are calculated by the Voigt–Reuss–Hill approximation. The relevant elastic tensors B_V, B_R, B, G_V, G_R and G under pressures are also listed in Table 3. The obtained bulk and shear modulus (421.3 and 301.7 GPa respectively) are in good agreement with that in Ref. 11). Moreover, they are much higher than that in hexagonal WN_2.[10] Therefore, tetragonal WN_2 possess superior elastic property to hexagonal structures, which were considered as the most stable structure in WN_2.[9] What most interested us is that the computed shear moduli of tetragonal WN_2 exceed those of all transition metal dinitrides synthesized. High shear modulus is helpful to their mechanical strength and also makes them candidates of superhard materials.

The ratio of bulk to shear modulus B/G is proposed as an indication of ductile and brittle character. The bulk modulus B is a factor that indicates the resistance to volume change by applied pressure, while the shear modulus G represents the resistance to plastic deformation. A high B/G ratio is associated with ductility, whereas a low value corresponds to brittle nature. If $B/G > 1.75$, the material behaves in a ductile manner; otherwise, the material behaves in a brittle manner. In addition, the ratio B/G reflects the hardness of a material. The smaller the ratio B/G is, the bigger the hardness of the material. The relation of B/G and pressure in WN_2 is exhibited in Fig. 2(a). When pressure increases from 0 to 240 GPa, the value of B/G changes from 1.396 to 2.801. It indicated that tetragonal WN_2 is a potential superhard material. Meanwhile, it is found that the ration of B/G is less than 1.75 below 66.2 GPa. The results indicated that the tetragonal WN_2 is prone to brittleness at low pressure, and is strongly prone to ductility at high pressure.

As is known, for tetragonal crystals the mechanical stability under isotropic pressure can be judged from the following criterion:[27,28)]

$$\tilde{C}_{11} - \tilde{C}_{12} > 0,\ \tilde{C}_{11} + \tilde{C}_{33} - 2\tilde{C}_{13} > 0,$$
$$\tilde{C}_{ii} > 0,\ 2\tilde{C}_{11} + \tilde{C}_{33} + 2\tilde{C}_{12} + 4\tilde{C}_{13} > 0 \tag{12}$$

in which $\tilde{C}_{\alpha\alpha} = C_{\alpha\alpha} - P$ ($\alpha = 1, 3, 4, 6$), $\tilde{C}_{12} = C_{12} + P$, $\tilde{C}_{13} = C_{13} + P$. By fitting $\tilde{C}_{44}$ data to second-order polynomials, we have the following relations:

$$\tilde{C}_{44} = \alpha + \beta P - \gamma P^2. \tag{13}$$

Figure 2(b) shows $\tilde{C}_{44}$ versus pressures for WN_2. When the pressure $\tilde{C}_{44} > 0$ is no longer fulfilled, indicating that tetragonal structure in WN_2 is not mechanical stable above pressure about 232.1 GPa. The result consists with that reported by Li *et al.*[11)]

Table 2 The elastic constants C_{ij} (GPa) for the tetragonal WN_2 at zero temperature and zero pressure.

	C_{11}	C_{33}	C_{44}	C_{66}	C_{12}	C_{13}
Present	956.7	954.7	222.2	315.1	117.0	172.7
LDA[11)]	955	973	231	324	136	176
GGA[11)]	853	861	203	276	122	147

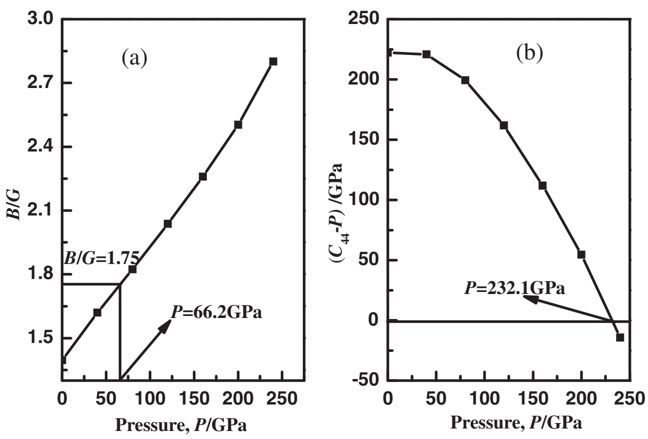

Fig. 2 (a) B/G (b) $C_{44} - P$ versus pressures.

Table 3 Zero temperature elastic constants C_{ij} (GPa) of tetragonal WN_2 under pressure P (GPa).

P	C_{11}	C_{33}	C_{44}	C_{66}	C_{12}	C_{13}	B_V	B_R	B	G_V	G_R	G
0	956.7	954.7	222.2	315.1	117.0	172.7	421.5	421.2	421.3	312.3	291.1	301.7
40	1218.7	1205.8	260.9	436.2	230.2	303.8	591.0	590.6	590.8	378.6	350.8	364.7
80	1450.2	1427.4	279.4	546.6	337.4	430.2	747.0	746.6	746.8	429.7	389.4	409.5
120	1663.2	1629.8	281.8	649.3	441.4	557.1	896.3	895.8	896.1	469.3	410.1	439.7
160	1865.9	1823.8	271.8	745.3	549.4	671.7	1037.9	1037.5	1037.7	501.9	416.7	459.3
200	2056.7	2010.9	254.6	835.9	657.0	787.7	1176.6	1176.2	1176.4	528.5	411.4	469.9
240	2240.4	2188.6	225.7	923.2	767.0	900.3	1311.6	1311.3	1311.4	548.4	387.9	468.2

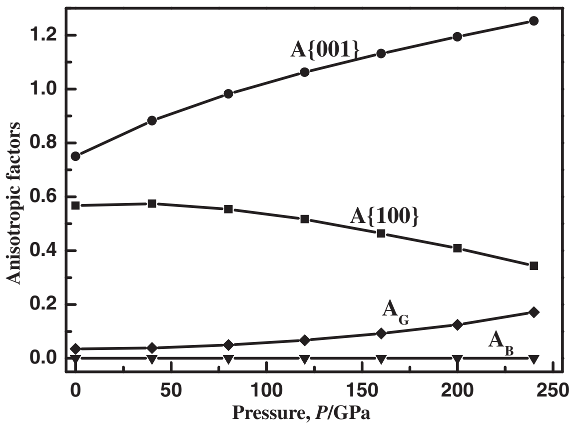

Fig. 3 Anisotropic factors of the tetragonal WN_2 as a function of pressure.

It is well known that microcracks are induced in alloys owing to the anisotropy of the coefficient of thermal expansion as well as elastic anisotropy. Hence it is important to calculate elastic anisotropy in superhard materials in order to understand these properties and hopefully find mechanisms which will improve their hardness and durability. A proper description of anisotropic behavior has an important implication in engineering science as well as in crystal physics. The shear anisotropic factors provide a measure of the degree of anisotropy in bonding between atoms in different planes. The shear anisotropic factors along {100} and {001} shear planes is defined as follows:[29)]

$$A_1 = A_{\{100\}} = \frac{4C_{44}}{C_{11} + C_{33} - 2C_{13}} \tag{14}$$

$$A_2 = A_{\{001\}} = \frac{2C_{66}}{C_{11} - C_{12}} \tag{15}$$

In the case of an isotropic crystal, the factors A_1, A_2 must be equal to one, while any value smaller or greater than one is a measure of the degree of elastic anisotropy possessed by the crystal. The anisotropic factors A_1, A_2 with pressure are plotted in Fig. 3. There is no experimental data to verify our results under pressure. When the applied pressure increases from 0 to 240 GPa, the anisotropic factors A_1, A_2 change by 39.5 and 66.9%, respectively, i.e., A_1 decreases quickly and A_2 increases sharply with increasing pressure, which is due to the fact that the elastic constants C_{11}, C_{33}, C_{66}, C_{12} and C_{13} increase by pressure. However, C_{44} slightly increases and decreases with pressure, which leads to the shear elastic anisotropy along {100} decreases under pressure. For this model, the elastic anisotropy is independent of the symmetry of the crystal only. In Fig. 1, we found that the ratio c/a changes with different pressure, that is, the structure is always varying with the applied pressure. Therefore, the elastic anisotropy may be different with pressure. These behaviors may be corresponding to the bonding situations in tetragonal WN_2, which is characterized as a strong cohesive bonding between pure N layers and a weaker bonding in the W and N layer.

In addition, the percentage elastic anisotropy for bulk modulus A_B and shear modulus A_G in polycrystalline materials can also be used as follows:

$$A_B = \frac{B_V - B_R}{B_V + B_R}, \quad A_G = \frac{G_V - G_R}{G_V + G_R} \tag{16}$$

where B and G denote the bulk and shear modulus, and the subscripts V and R represent the Voigt and Reuss approximations. The percentage of bulk and shear anisotropies, i.e., A_B and A_G are also obtained and presented in Fig. 3. It shows that tetragonal WN_2 is largely isotropic in bulk and slightly anisotropic in shear at pressures or not.

4. Conclusions

The elastic properties and anisotropies of tetragonal WN_2 under high pressure are investigated by means of the *ab initio* plane wave pseudopotential density functional theory within the local density approximation (LDA). The equilibrium lattice parameters and volume is obtained. The dependence of the elastic constants and the aggregate elastic moduli (B, G) of tetragonal WN_2 under high pressure from 0 to 240 GPa are also presented. But as far as we know, there are no experimental data available for these quantities. Thanks to availability of the complete elastic tensor it is possible to obtain anisotropy factors for the crystal. The systematic increases of the anisotropy with pressure are observed except symmetry plane {100}. From our analysis, we also find that WN_2 is a brittle system below about 66 GPa, whereas it becomes ductile at higher pressures. Moreover, from our elastic constants of WN_2 under pressure, we have found that WN_2 becomes more ductile with the pressure increasing. By the elastic stability criteria, it is predicted that tetragonal WN_2 are not stable above 232.1 GPa. The present theoretical results should be used to stimulate future experimental and theoretical work.

Acknowledgements

This work was financially supported by the National Natural Science Foundation of China (Grant Nos. 11147101 and 11071107), the Henan Research Program of Basic and Frontier Technology under Grant No. 102300410213 and Henan Science and Technology Agency of China under Grant No. 122102210390, the Henan Natural Science Basic Research under Grant No. 2011B140013 and the Scientific Research Foundation of Luoyang Normal University under Grant No. 2010-QNJJ-003.

REFERENCES

1) A. Šimůnek and J. Vackář: Phys. Rev. Lett. **96** (2006) 085501 1–4.
2) E. Gregoryanz, C. Sanoup, M. Somayazulu, J. Badro, G. Fiquet, H. K. Mao and R. J. Hemley: Nat. Mater. **3** (2004) 294–297.
3) J. C. Crowhurst, A. F. Goncharov, B. Sadigh, C. L. Evans, P. G. Morrall, J. L. Ferreira and A. J. Nelson: Science **311** (2006) 1275–1278.
4) A. F. Young, C. Sanloup, E. Gregoryanz, S. Scandolo, R. J. Hemley and H. K. Mao: Phys. Rev. Lett. **96** (2006) 155501 1–4.
5) R. Yu, Q. Zhan and X. F. Zhang: Appl. Phys. Lett. **88** (2006) 051913–051915.
6) R. Yu, Q. Zhan and L. C. De Jonghe: Angew. Chem. Int. Ed. **119** (2007) 1154–1158.
7) P. Kroll, T. Schröter and M. Peters: Angew. Chem. Int. Ed. **44** (2005) 4249–4254.

8) Q. Li, H. Wang and Y. M. Ma: J. Superhard. Mater. **32** (2010) 192–204.
9) H. Wang, Q. Li, Y. W. Li, Y. Xu, T. Cui, A. R. Oganov and Y. M. Ma: Phys. Rev. B **79** (2009) 132109 1–4.
10) X. F. Li, Z. L. Liu, C. L. Ding and G. F. Ji: Mater. Chem. Phys. **130** (2011) 14–19.
11) X. P. Du, Y. X. Wang and V. C. Lo: Phys. Lett. A **374** (2010) 2569–2574.
12) V. Milman, B. Winkler, J. A. White, C. J. Packard, M. C. Payne, E. V. Akhmatskaya and R. H. Nobes: Int. J. Quantum Chem. **77** (2000) 895–910.
13) D. Vanderbilt: Phys. Rev. B **41** (1990) 7892–7895.
14) S. H. Vosko, L. Wilk and M. Nussair: Can. J. Phys. **58** (1980) 1200–1211.
15) J. H. Wang, S. Yip, S. R. Phillpot and D. Wolf: Phys. Rev. B **52** (1995) 12627–12635.
16) D. C. Wallace: *Thermodynamics of Crystals*, (Wiley, New York, 1972).
17) B. B. Karki, G. J. Ackland and J. Crain: J. Phys.: Condens. Matter **9** (1997) 8579–8589.
18) T. H. K. Barron and M. L. Klein: Proc. Phys. Soc. **85** (1965) 523–532.
19) W. Voigt: *Lehrbuch der Kristallphysik*, (Leipzig, Taubner, 1928).
20) A. Reuss: Z. Angew. Math. Mech. **9** (1929) 55–66.
21) R. Hill: Proc. Soc. London A **65** (1952) 350–362.
22) F. D. Murnaghan: Proc. Natl. Acad. Sci. USA **30** (1944) 244–247.
23) K. E. Spear: J. Am. Ceram. Soc. **72** (1989) 171–191.
24) F. Occelli, D. L. Farber and R. L. Toullec: Nat. Mater. **2** (2003) 151–154.
25) Y. X. Wang: Appl. Phys. Lett. **91** (2007) 101904–101906.
26) Y. X. Wang, M. Arai and T. Sasaki: Appl. Phys. Lett. **90** (2007) 061922–061924.
27) Z. J. Wu, E. J. Zhao, H. P. Xiang, X. F. Hao, X. J. Liu and J. Meng: Phys. Rev. B **76** (2007) 054115–054129.
28) G. V. Sinko and N. A. Smirnow: J. Phys.: Condens. Matter **14** (2002) 6989–7006.
29) P. Ravindran, L. Fast, P. A. Korzhayi and B. Johansson: J. Appl. Phys. **84** (1998) 4891–4904.